doi:10.1093/brain/awaa431 BRAIN 2021: 144; 1–4 | e18

BRAIN
A JOURNAL OF NEUROLOGY

LETTER TO THE EDITOR

MN1 gene loss-of-function mutation causes cleft palate in a pedigree

Li Shu,[1,2,3] Dinghua He,[4] Dan Wu,[4] Ying Peng,[1] Hui Xi,[1] Xiao Mao[1,2,†] and Hua Wang[1,2,†]

[†]These authors contributed equally to this work.

1 Department of Medical Genetics, Maternal and Child Health Hospital of Hunan Province, Changsha, China
2 National Health Commission Key Laboratory of Birth Defects Research, Prevention and Treatment, Hunan Provincial Maternal and Child Health Care Hospital, Changsha, China
3 Department of School of Life Sciences, Central South University, Changsha, China
4 Department of Otorhinolaryngology, Maternal and Child Health Hospital of Hunan Province, Changsha, China

Correspondence to: Hua Wang
Department of Medical Genetics, Maternal and Child Health Hospital of Hunan Province, Changsha, China
E-mail: wanghua_213@hotmail.com

Correspondence may also be addressed to: Xiao Mao
E-mail: gbtechies@outlook.com

We read with great interest the article entitled '*MN1* C-terminal truncation syndrome is a novel neurodevelopmental and craniofacial disorder with partial rhombencephalosynapsis' published in *Brain* by Mak *et al.* (2020). They reported 22 patients with CEBALID syndrome who showed severe symptoms including global developmental delay, craniofacial and brain abnormalities. All of these patients carried *MN1* heterozygous C-terminal mutations which may have a dominant-negative or gain-of-function effect.

MN1 (MIM 156100) was initially identified to be disrupted by balanced chromosomal translocation and play a role in meningioma and myeloproliferative diseases (Buijs *et al.*, 1995; Lekanne Deprez *et al.*, 1995). There were no *MN1*-related phenotypes established in humans until Mak *et al.* first described the gene as a causative gene for *MN1* C-terminal truncation (MCTT) syndrome-CEBALID syndrome (MIM 618774) in 2020. They found that these mutations lay in exon 2 or 3′ of exon 1 and were predicted to escape from the nonsense-mediated mRNA decay (NMD) (Mak *et al.*, 2020). Miyake *et al.* (2020) also reported three patients carrying *MN1* C-terminal mutations with similar severe clinical features. They proved that aberrant truncated MN1 proteins acted in a gain-of-function manner by increasing protein stability, inhibiting cell proliferation and enhancing MN1 nuclear aggregation (Miyake *et al.*, 2020).

Although the mutations in the N-terminus of the gene were predicted to cause the distinct clinical features due to MN1 haploinsufficiency, functional studies were not performed on mechanisms underlying the milder *MN1*-related phenotype. In support and to supplement the message of this paper, our study identified a mutation located outside the C-terminal region of *MN1* in a Chinese pedigree and performed expression experiments for the first time.

We identified a heterozygous frameshift deletion variant in two patients in a Chinese pedigree. Proband whole exome sequencing was conducted and variants were validated by Sanger sequencing in other members in the pedigree including the parents (Subjects II-1 and II-2), the aunt (Subject II-3), and the maternal grandparents (Subjects I-1 and I-2). A frameshift deletion located in the middle of *MN1* exon 1 [NM_002430.3:c.2253del, p.G752Afs*12 (chr22: 27798291-27798291)] was identified resulting in a complete co-segregation within the pedigree (Fig. 1A and B). All participants signed informed consent forms, and the study was approved by the ethics committee of the Maternal and Child Health Hospital of Hunan Province (2020-S003).

The two patients showed similar clinical phenotypes as cleft palate and conductive hearing loss. No severe clinical phenotypes in CEBALID syndrome were observed including developmental delay, craniofacial features or characteristic

Advance access publication December 22, 2020
© The Author(s) (2020). Published by Oxford University Press on behalf of the Guarantors of Brain.
This is an Open Access article distributed under the terms of the Creative Commons Attribution Non-Commercial License (http://creativecommons.org/licenses/by-nc/4.0/), which permits non-commercial re-use, distribution, and reproduction in any medium, provided the original work is properly cited. For commercial re-use, please contact journals.permissions@oup.com

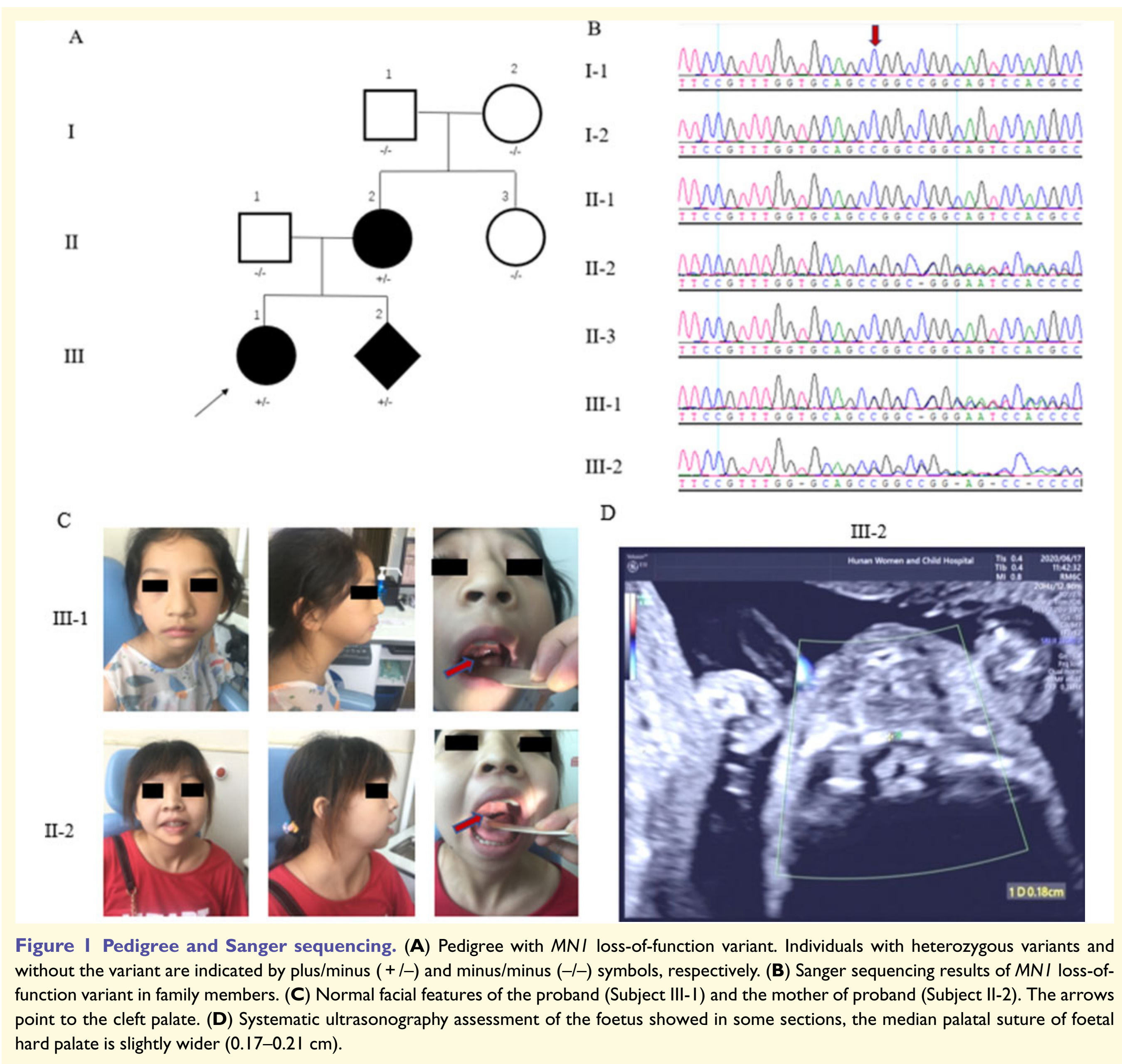

Figure 1 Pedigree and Sanger sequencing. (**A**) Pedigree with *MN1* loss-of-function variant. Individuals with heterozygous variants and without the variant are indicated by plus/minus (+/–) and minus/minus (–/–) symbols, respectively. (**B**) Sanger sequencing results of *MN1* loss-of-function variant in family members. (**C**) Normal facial features of the proband (Subject III-1) and the mother of proband (Subject II-2). The arrows point to the cleft palate. (**D**) Systematic ultrasonography assessment of the foetus showed in some sections, the median palatal suture of foetal hard palate is slightly wider (0.17–0.21 cm).

brain imaging (Mak *et al.*, 2020). The proband (Subject III-1) is a 9-year-old female, born at full term (38 weeks) following a normal pregnancy. Cleft palate was present at birth and at the age of 1.5 years, cleft palate repair surgery was carried out (Fig. 1C). The mother of the proband (Subject II-2) is a 30-year-old female, born at full term (40 weeks) following a normal pregnancy. Cleft palate was present at birth and repair surgery was carried out at 22 years of age (Fig. 1C).

Pure tone audiometry (PTA) (Supplementary Fig. 1), tympanometry (Supplementary Fig. 2) and acoustic reflex testing (Supplementary Fig. 3) of the two patients (Subjects III-1 and II-2) showed conductive hearing loss, suggesting the presence of external and middle ear lesions or functional abnormalities. Physical examination of the ear showed that external auditory canals were patent and tympanic membranes were intact in both patients. The proband and the mother of the proband were of normal intelligence with IQ scores of 96 and 93, respectively. Brain MRI was normal.

At 23 weeks of a second pregnancy the systematic ultrasonography assessment of the foetus showed sonographic changes of palatal suture in the foetal hard palate (Fig. 1D). No other dysmorphism or developmental delay was observed in the foetus. Invasive prenatal diagnosis by amniocentesis was performed and Sanger sequencing was performed to detect the variant. The same variant in *MN1* was identified (Fig. 1B).

To confirm the pathogenesis of the variant in *MN1*, *in vitro* functional expression studies were performed on peripheral blood lymphocytes of patients and controls in the

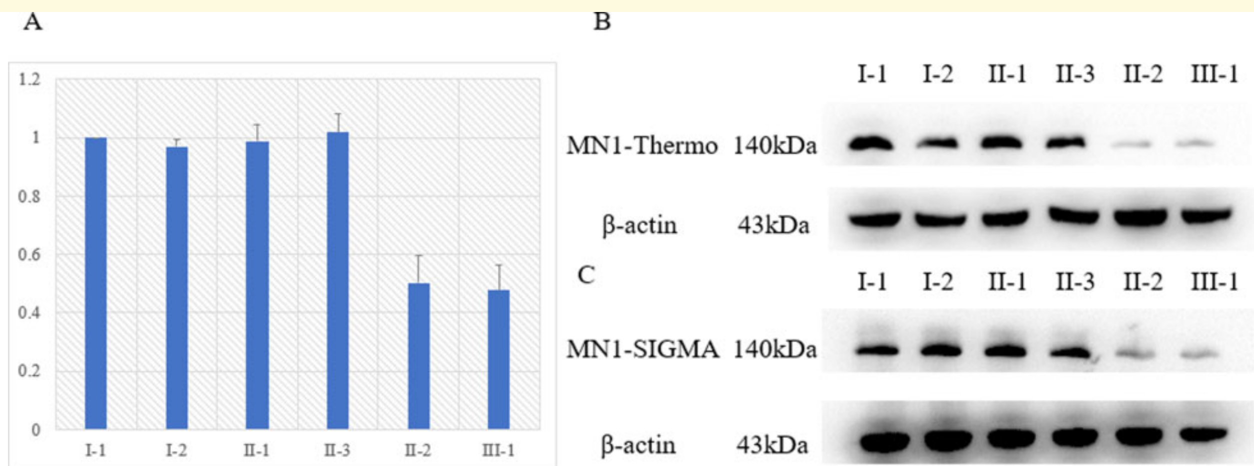

Figure 2 Expression level analyses. (**A**) RT-PCR analysis showed decreased *MN1* mRNA expression level in patients compared to controls in lymphocytes. β-Actin mRNA was used as an internal control for normalization and quantitative analysis of *MN1* mRNA levels. $P < 0.01$, Student's *t*-test. (**B**) Western blot analysis showing that MN1 protein levels were decreased in patients compared with control subjects.

pedigree. Lymphocytes were separated from blood using lymphocyte isolation solution (Ficoll® Paque Plus 17-1440-02). Quantitative real-time PCR (RT-PCR) was used to analyse the RNA expression of *MN1*. Briefly, total mRNA was prepared for RT-PCR using a RNeasy® Mini Kit (Qiagen) and cDNA was synthesized with the AMV First Strand cDNA Synthesis Kit (SK2445). The sequences of primers were *MN1*-F, 5′-GCTTTCCGTTTGGTGCAG-3′; *MN1*-R, 5′-TGGAAATCAGGCTGCGG-3′; b-actin-F, 5′-TAGTTGCGTTACACCCTTTCTTG-3′; and b-actin-R , 5′-TCACCTTCACCGTTCCAGTTT-3′. RT-PCR was carried out using SYBR™ Green PCR master mix (Applied Biosystems) according to the manufacturer's instructions. PCR amplifications (40 cycles at 95°C for 15 s and 57°C for 20 s) were performed using an ABI 7900 (Applied Biosystems). The average Ct values calculated from quadruplicate PCR reactions were normalized to the average Ct values for β-actin (*ACTB*). The normalized values were used to calculate the expression of MN1 relative to the controls using the ΔΔCt method. RT-PCR analysis showed significantly reduced levels of mRNA expression in two patients (Subjects II-2 and III-1) compared with unaffected control subjects (Subjects I-1, I-2, II-1 and II-3) in the pedigree (Fig. 2A), suggesting NMD-mediated mRNA degradation of MN1 mRNA.

Western blot was carried out to analyse MN1 protein. Total proteins were extracted by RIPA buffer (Biosesang) and subjected to the regular western blot procedure. Antibodies used for the determination of MN1 protein included anti-MN1 (1:1000, SAB4501908, Sigma), anti-MN1 (1:1000, PA5-38666, ThermoFisher), anti-β-actin (1:2000), and anti-Rabbit IgG (1:5000, Sigma-Aldrich). Enhanced chemiluminescence (ECL) plus western blotting substrate (Thermo Scientific) was used for detection of protein bands. The level of MN1 protein detected in two patients (Subjects II-2 and III-1) was significantly lower than in four unaffected individuals (Subjects I-1, I-2, II-1 and II-3) in the pedigree (Fig. 2B) suggesting an MN1 haploinsufficiency caused by *MN1* loss-of-function mutation.

The *MN1* gene comprises two exons and encodes a 1320 amino acid protein; exon 1 encodes amino acids 1–1260 and exon 2 encodes the remaining 60 C-terminal amino acids. Deletions, including the whole gene sequence of *MN1*, have been reported previously to be associated with variable clinical phenotypes including neurodevelopmental anomalies, facial dysmorphisms, congenital heart defects, etc. (Said *et al.*, 2011; Davidson *et al.*, 2012; Breckpot *et al.*, 2016; Mak *et al.*, 2020). However, these deletions contained many MIM genes and it is difficult to judge the gene contributions. Until 2020, the truncating variants in the C-terminal region of the gene were recognized to cause a specific disease—CEBALID syndrome—which was characterized by CNS and craniofacial skeletal development disorders (Mak *et al.*, 2020). Most of the heterozygous variants associated with CEBALID syndrome were *de novo* mutations, except for one family in which two affected brothers inherited the mutation from a mildly affected father who carried a somatic mosaic mutation. In the same year, a functional study revealed that the C-terminal variants escaped the NMD system and increased the amount of mutant MN1 protein, which could explain the severe clinical manifestations of the syndrome (Miyake *et al.*, 2020).

The molecular mechanism by which loss-of-function mutations of *MN1* lead to mild clinical features in the patients is not known. In our study, we first identified a loss-of-function variant located in the middle of exon 1 in two patients in a pedigree and proved that *MN1* causes a mild phenotype of disease by NMD leading to MN1 haploinsufficiency by expression experiments. The heterozygous *Mn1* knockout mice showed an intermediate phenotype with hypoplastic membranous bone and incomplete penetrance of the cleft palate when compared to homozygous knockout *Mn1*

(Meester-Smoor *et al.*, 2005). Therefore, combined with the former research on C-terminal *MN1* variants, the clinical severity of patients carrying *MN1* variants may be related to a dosage effect of the MN1 protein. The truncated MN1 protein is a transcriptional cofactor and the mutant protein could impair the binding with transcription factors and cause dysregulation of target genes (Meester-Smoor *et al.*, 2005; Miyake *et al.*, 2020). It is plausible that the distinct clinical phenotypes determined by different regions of *MN1* were through regulation of corresponding downstream genes (Lai *et al.*, 2014). It has been reported that *MN1* may interplay with transcription factors regulating palate development genes such as Tbx22 (Liu *et al.*, 2008). Our study adds to the growing evidence of genotype-phenotype correlations of *MN1* and provides clues for future mechanism research on *MN1* loss-of-function variants.

Data availability

The data that support the findings of this study are available from the corresponding author, upon reasonable request.

Competing interests

The authors report no competing interests.

Funding

This work was supported by the National Natural Science Foundation of China (grant number 81801136), Hunan Provincial Major Science and Technology Project (grant number 2019SK1010) and the China Postdoctoral Science Foundation (2019M662804).

Supplementary material

Supplementary material is available at *Brain* online.

References

Breckpot J, Anderlid BM, Alanay Y, Blyth M, Brahimi A, Duban-Bedu B, et al. Chromosome 22q12.1 microdeletions: confirmation of the MN1 gene as a candidate gene for cleft palate. Eur J Hum Genet 2016; 24: 51–8.

Buijs A, Sherr S, van Baal S, van Bezouw S, van der Plas D, Geurts van Kessel A, et al. Translocation (12; 22) (p13; q11) in myeloproliferative disorders results in fusion of the ETS-like TEL gene on 12p13 to the MN1 gene on 22q11. Oncogene 1995; 10: 1511–9.

Davidson TB, Sanchez-Lara PA, Randolph LM, Krieger MD, Wu SQ, Panigrahy A, et al. Microdeletion del(22)(q12.2) encompassing the facial development-associated gene, MN1 (meningioma 1) in a child with Pierre-Robin sequence (including cleft palate) and neurofibromatosis 2 (NF2): a case report and review of the literature. BMC Med Genet 2012; 13: 19.

Lai CK, Moon Y, Kuchenbauer F, Starzcynowski DT, Argiropoulos B, Yung E, et al. Cell fate decisions in malignant hematopoiesis: leukemia phenotype is determined by distinct functional domains of the MN1 oncogene. PLoS One 2014; 9: e112671.

Lekanne Deprez RH, Riegman PH, Groen NA, Warringa UL, van Biezen NA, Molijn AC, et al. Cloning and characterization of MN1, a gene from chromosome 22q11, which is disrupted by a balanced translocation in a meningioma. Oncogene 1995; 10: 1521–8.

Liu W, Lan Y, Pauws E, Meester-Smoor MA, Stanier P, Zwarthoff EC, et al. The Mn1 transcription factor acts upstream of Tbx22 and preferentially regulates posterior palate growth in mice. Development 2008; 135: 3959–68.

Mak CCY, Doherty D, Lin AE, Vegas N, Cho MT, Viot G, et al.; University of Washington Center for Mendelian Genomics. MN1 C-terminal truncation syndrome is a novel neurodevelopmental and craniofacial disorder with partial rhombencephalosynapsis. Brain 2020; 143: 55–68.

Meester-Smoor MA, Vermeij M, van Helmond MJ, Molijn AC, van Wely KH, Hekman AC, et al. Targeted disruption of the Mn1 oncogene results in severe defects in development of membranous bones of the cranial skeleton. Mol Cell Biol 2005; 25: 4229–36.

Miyake N, Takahashi H, Nakamura K, Isidor B, Hiraki Y, Koshimizu E, et al. Gain-of-function MN1 truncation variants cause a recognizable syndrome with craniofacial and brain abnormalities. Am J Hum Genet 2020; 106: 13–25.

Said E, Cuschieri A, Vermeesch J, Fryns JP. Toriello-Carey syndrome with a 6Mb interstitial deletion at 22q12 detected by array CGH. Am J Med Genet A 2011; 155: 1390–2.